Using distributions and stable isotopes of *n*-alkanes to disentangle organic matter contributions to sediments of Laguna Potrok Aike, Argentina

Katja Hockun [a] *, Gesine Mollenhauer [b], Sze Ling Ho [c, d], Jens Hefter [b], Christian Ohlendorf [e], Bernd Zolitschka [e], Christoph Mayr [f, g], Andreas Lücke [h], Enno Schefuß [a]

[a] *MARUM – Center for Marine Environmental Sciences, University of Bremen, Leobener Straße, 28359 Bremen, Germany*

[b] *Alfred-Wegener-Institut Helmholtz - Zentrum für Polar- und Meeresforschung, Am Handelshafen 12, 27570 Bremerhaven, Germany*

[c] *Alfred-Wegener-Institut Helmholtz - Zentrum für Polar- und Meeresforschung, Telegrafenberg A43, 14473 Potsdam, Germany*

[d] *Department of Earth Science, University of Bergen and Bjerknes Centre for Climate Research, Allégaten 41, 5007 Bergen, Norway*

[e] *Geomorphology and Polar Research (GEOPOLAR), Institute of Geography, University of Bremen, Celsiusstr. FVG-M, D-28359 Bremen, Germany*

[f] *Institute of Geography, Friedrich-Alexander-Universität Erlangen-Nürnberg, Wetterkreuz 15, D-91058 Erlangen, Germany*

[g] *Paleontology & Geobiology and GeoBio-Center, Ludwig-Maximilians-Universität München, Richard-Wagner-Str. 10, D-80333 München, Germany*

*Corresponding author Tel.: +49 173 7522278;
E-mail address: khockun@marum.de

[h] *Institute of Bio- and Geosciences, IBG-3: Agrosphere, Research Center Jülich, D-52428 Jülich, Germany*

ABSTRACT

When using biomarkers such as *n*-alkanes as tools for paleo-environmental reconstructions, it is imperative to determine their specific sources for each setting. Towards that goal, we analysed a set of various potential organic matter (OM) sources such as aquatic and terrestrial plants, dust, and soils from Laguna Potrok Aike (LPA) and surrounding areas in Southern Patagonia. We determined chain length distributions and hydrogen (δD) and carbon ($\delta^{13}C$) isotopic compositions of *n*-alkanes of different OM sources in order to quantify their relative contributions to lake sediments. Our results reveal that mid-chain *n*-alkane, n-C_{23}, is predominantly produced by submerged aquatic plants, whereas long-chain *n*-alkanes (n-C_{29} to n-C_{31}) are derived from various terrestrial sources. We estimated their relative contributions to the sediment using two approaches, i.e. based on the *n*-alkane distributions and their δD and $\delta^{13}C$ values. Both approaches result in similar estimates of aquatic and terrestrial contributions for mid- and long-chain *n*-alkanes to the sediment. 62-73% of the mid-chain n-C_{23} alkanes originate from aquatic sources while 66-77% of the long-chain *n*-alkanes originate from dust and 14-30% from terrestrial plants. Our study shows

that mid-chain *n*-alkanes such as *n*-C_{23} alkane in LPA are derived mainly from aquatic macrophytes and thus have the potential to record changes in lake-water isotopic composition. In contrast, the *n*-C_{29} alkane reflects the isotopic signal of various terrestrial sources from Southern Patagonia.

Keywords: ICDP, PASADO, *n*-alkanes, hydrogen (δD) and carbon ($\delta^{13}C$) isotopes

1. Introduction

Southern Patagonia is a key location for paleo-environmental reconstruction since it is the southernmost ice-free landmass strongly influenced by the Southern Hemispheric Westerlies (SHW). Their position and intensity is thought to influence global deep-water circulation and thus other climate-controlling factors, such as exchange of carbon dioxide with the atmosphere (Anderson et al., 2009; Mayr et al., 2013). To investigate past climatic changes in the southern mid-latitudes, the ICDP drilling campaign PASADO retrieved a 100-m long lacustrine sediment core from Laguna Potrok Aike (LPA) in 2008. The core spans the last ca. 51,000 years (Kliem et al., 2013) and enabled various multiproxy investigations to study past environmental and climate changes in Southern Patagonia, such as pollen studies (Wille et al., 2007; Schäbitz et al., 2013), diatom studies (Massaferro et al., 2012; Recasens et al., 2015; Zimmermann et al., 2015),

isotopic reconstructions (Mayr et al., 2009; J. Zhu et al., 2013, 2014a; Oehlerich et al., 2015) and others (Zolitschka et al., 2013). A previous study used bulk organic $\delta^{13}C$ and $\delta^{15}N$ to distinguish organic matter (OM) sources in and around LPA to identify the sources of sedimentary OM (Mayr et al., 2009). We followed a similar approach by using *n*-alkanes as specific tracers for OM sources.

The source of *n*-alkanes in sedimentary archives may be inferred from their distinct chain lengths. While mid-chain *n*-alkanes with 23 and 25 carbon atoms (n-C_{23}, n-C_{25}) are inferred to be predominantly derived from submerged aquatic plants (Ficken et al., 2000) and *Sphagnum* species (Baas et al., 2000; Bush and McInerney, 2013), long-chain *n*-alkanes with 27 to 31 carbon atoms (n-C_{27}–C_{31}) are thought to be mainly produced by terrestrial higher plants (Eglinton and Hamilton, 1967). Some recent studies, however, suggested that terrestrial higher plants also produce small amounts of mid-chain compounds (Gao et al., 2011; Liu et al., 2015), while aquatic plants might also contribute long-chain *n*-alkanes (Ficken et al. 2000; Aichner et al. 2010a; Liu et al. 2015).

The carbon stable isotope composition ($\delta^{13}C$) of *n*-alkanes reflects the different carbon sources, their isotopic compositions, and biosynthetic pathways of their producers. For instance, the availability of dissolved CO_2 and HCO_3^- in lake ecosystems is reflected in the $\delta^{13}C$ values of mid-chain *n*-alkanes from aquatic plants (Ficken et al., 2000), whereas $\delta^{13}C$ values of the long-chain *n*-alkanes enables to distinguish relative OM contributions by C3

and C4 plants in regions with occurrence of both photosynthetic carbon fixation pathways (e.g. Magill et al., 2013). Vegetation in Southern Patagonia, however, consists solely of C_3 plants (Mayr et al., 2009; Pfadenhauer and Klötzli, 2015). Therefore, changes in $\delta^{13}C$ ratios of long-chain *n*-alkanes likely reflect changes in water stress of C_3 plants (Dawson et al., 2002). The hydrogen stable isotope (δD) composition of mid-chain *n*-alkanes from aquatic plants is presumed to reflect the lake water hydrogen isotopic composition (Mügler et al., 2009; Aichner et al., 2010a; Schmidt et al., 2014), whereas the δD values of long-chain *n*-alkanes serve as indicator for isotopic composition of precipitation and contain information about changes in humidity and evapotranspiration (Sachse et al., 2004; Schefuß et al., 2005; Mügler et al., 2008; Aichner et al., 2010b; Sachse et al., 2012).

For a reliable reconstruction of climate changes based on *n*-alkane isotope compositions, a well-constrained understanding of their sources in each setting is required. Therefore, we analyzed terrestrial plants, material from dust traps, topsoil samples from the LPA catchment and from an E-W transect, aquatic plant samples, and exposed and recent lake sediments from LPA, for their *n*-alkane distributions and compound-specific ($\delta^{13}C$ and δD) isotopes. The goal of this research is to evaluate the reliability of the individual sedimentary *n*-alkanes as source-specific paleo-environmental indicators and for future investigation on the PASADO core. In addition, we compare two quantitative methods, which may be a useful approach to

constrain the determination of the source of sedimentary *n*-alkanes and thereby also paleo-environmental reconstructions based on them.

2. Study Site

Laguna Potrok Aike (51°58′ S, 70°23′ W, Fig. 1) is an almost circular maar lake located in the Pali Aike Volcanic Field in Southern Patagonia. The 0.77 Ma old crater hosts a lake with a maximum diameter of 3470 m and a catchment area of about 200 km² (Zolitschka et al., 2006, 2013). In 2002, the lake level was recorded at 112 m above sea level and maximum water depth was 100 m (Wille et al., 2007). Monitoring data of lake-level fluctuations show inter-annual differences of 1-2 m. LPA is a terminal sub-saline lake, with a water balance mainly controlled by precipitation, groundwater inflow and the rate of evaporation (Zolitschka et al., 2006).

Present-day climate at LPA is dominated by a strong influence of the SHW. Westerly winds reach mean annual wind speeds of 7.4 m s^{-1} (Endlicher, 1993). The climate is semi-arid with an annual mean precipitation of around 200 mm (Ohlendorf et al., 2013) and a mean annual temperature of 7.4 °C (Zolitschka et al., 2006).

The distribution of vegetation in southern South America depends on the amount of precipitation in the region and is divided in five major vegetation zones: Magellanic moorland close to the Pacific coast, evergreen Magellanic rain forest of the Andes, deciduous *Nothofagus* forest near the tree line and

east of the Andes, Andean tundra above the tree line and Patagonian steppe east of the tree line (Hueck and Seibert, 1981; Moore, 1983; Roig, 1998), Most of the Pali Aike Volcanic Field, including the area around LPA, is covered by sparse vegetation of the Patagonian steppe mainly characterized by the presence of tussock (*Festuca, Stipa*), short grasses (*Poa, Carex*) and shrubs (Peri et al., 2013). These plants use the C_3 photosynthetic pathway (Pfadenhauer and Klötzli, 2015). The zone in the range of short-term lake-level fluctuations is free of vegetation (Wille et al., 2007). The deeper littoral zone is covered by aquatic macrophytes, mainly *Potamogeton pectinatus* and *Myriophyllum* cf. *quitense*, at water depths between ca. 1.5 and 15 m (Wille et al., 2007).

3. Material and Methods

3.1. Sample Collection

The plant samples and five topsoil samples were collected during several field campaigns in February and March 2002, 2003 and 2004 (Mayr et al., 2009). The plant samples analysed in this study represent the predominant vegetation in the LPA catchment. Topsoil samples were collected from the uppermost centimeter of the soils. Additionally, 16 topsoil samples were taken every 20 km on an E-W transect along the Route 40 from Rio Gallegos to Rio Turbio (February and March 2011), (Figure 1) (Schäbitz et al., 2013).

During the same field campaign four dust traps (PT = pollen traps) were deployed and collected one year later. These pollen traps consisted of a plastic container with a diameter of about 20 cm and a glycerine-covered bottom. They were embedded in the ground and covered with a lid with open slits. In addition, two sediment traps with an active area of 55 cm^2 were deployed on a mooring string at 30 and 90 m water depth from March 2003 to March 2005 (Ohlendorf et al., 2013). Lacustrine surface sediment samples were recovered from 2002 to 2004 (Mayr et al., 2009), in 2005 (Kastner et al., 2010) and in 2009. During the sample collection in 2005 several gravity cores were taken and the mixed upper 10 cm are used for analysis in this study. Based on previous studies (Haberzettl et al., 2005; Kliem et al., 2013) the upper 10 cm of the LPA sediment are estimated to be 10 to 100 years old. All sampling locations and dates are listed in Supplementary Table 1. All samples were dried and stored in glass containers at room temperature, except a few plant samples which were stored in plastic bags or plastic tubes.

3.2. *Quantification and isotope analysis of n-alkanes*

All samples were freeze-dried and ground prior to extraction. An internal standard (squalane) was added to all samples to estimate the accuracy of the measurements. Between 2 to 7 g of sediment or soil and 0.2 to 0.5 g of

183 plant biomass were extracted via ultra-sonication using organic solvents of
184 decreasing polarity: methanol (MeOH), methanol/dichloromethane
185 (MeOH/DCM, 1:1, v/v) and DCM for 5 min each. Dust traps were extracted
186 via Soxhlet extraction with MeOH/DCM, 1:1, v/v for 48 h. Neutral lipids
187 were separated using Al_2O_3-column chromatography to separate polar from
188 apolar lipids. Subsequently, $AgNO_3$-silica gel column chromatography was
189 performed to separate saturated from unsaturated hydrocarbons in apolar
190 fractions. The *n*-alkanes were identified and quantified by gas
191 chromatography using an Agilent 7890A gas chromatograph with capillary
192 gas chromatography-flame ionization detection (GC-FID). An external
193 standard (Chiron, *n*-C_{10}-*n*-C_{40} alkanes, 2ng/µl) was used for the
194 identification and quantification of *n*-alkanes. Based on replicate analysis of
195 the external standard the precision of quantification is around 5%.
196
197 *3.2.1. Compound-specific carbon stable isotope analyses*
198
199 Carbon stable isotope ($\delta^{13}C$) compositions of *n*-alkanes were measured
200 using a Thermo Trace GC coupled to a Finnigan MAT 252 isotope-ratio
201 monitoring-mass spectrometer (irm-MS) via a modified Finnigan GC/C III
202 combustion interface operated at 1000 °C. CO_2 reference gas with known
203 isotopic composition was used for isotope calibration. $\delta^{13}C$ values are
204 reported in permil (‰) relative to Vienna Pee Dee Belemnite (VPDB).
205 Measurements were done at least in duplicate. An external standard

206 consisting of 16 *n*-alkanes with known $\delta^{13}C$ values measured between
207 samples reveals a long-term precision of 0.3 ‰ VPDB (average absolute
208 deviations from known values). The internal standard (squalane) yielded an
209 accuracy of 0.4 and a precision of 0.2 ‰ VPDB (n=84). Standard deviations
210 for replicates of all measured compounds are listed in Supplementary Table
211 2.
212
213 *3.2.2. Compound-specific hydrogen isotope analyses*
214
215 Compound-specific δD compositions were measured with a Thermo
216 Trace GC coupled to a Thermo Fischer Scientific MAT 253 irm-MS via a
217 pyrolysis reactor operated at 1420 °C. Measurements were calibrated
218 against H_2 reference gas with known isotopic composition. All δD values are
219 reported in ‰ relative to Vienna Standard Mean Ocean Water (VSMOW).
220 Samples were measured at least in duplicates. The H^{3+}-factor was
221 monitored daily and varied between 6.7 and 6.8 ppm nA^{-1}. An external
222 standard consisting of 16 *n*-alkanes with known δD values measured
223 between samples reveals a long-term precision of 3 ‰ VSMOW (average
224 absolute deviations from known values). The internal standard (squalene)
225 yielded accuracy and precision of 2 and 1 ‰ VSMOW (n=84), respectively.
226 Standard deviations for replicates of all measured compounds are listed in
227 Supplementary Table 3.
228

3.3. n-Alkane distribution parameters

The P_{aq} proxy (Ficken et al., 2000) provides a measure for the sedimentary input from submerged/floating aquatic plants relative to that from terrestrial plants and expresses the abundance of C_{23} and C_{25} *n*-alkanes relative to C_{29} and C_{31} homologues:

$$P_{aq} = (C_{23} + C_{25})/(C_{23} + C_{25} + C_{29} + C_{31}) \quad (1)$$

The average chain length (ACL) is the weighted average of the C_{23} to C_{33} *n*-alkanes:

$$ACL = \sum(C_n * n)/\sum C_n \quad (2)$$

(Poynter et al., 1989) where C is abundance and n ranges from 23 to 33.

3.4. Model approaches

To determine the fractional contribution of different *n*-alkane sources to the LPA sediment we applied two different model approaches. The first model is based on the *n*-alkane distributions and the second on their isotope compositions (Supplementary Tables 1, 2, 3). We assumed three sources/end-members for both models, i.e. aquatic plants, terrestrial plants and dust (justification in discussion 5.1.). End-member values are calculated as the mean of all samples within each source group (Supplementary Tables 1, 2, 3).

One the one hand we estimated the fractional contributions of *n*-alkanes from three sources using the model described by Gao et al. (2011). On the other hand we developed a linear three end-member mixing model based on the δD and $\delta^{13}C$ signals of the *n*-C_{23} and *n*-C_{29} alkanes to independently determine the relative contributions from three leaf wax sources (aquatic plants, terrestrial plants and dust) to the lake sediments. Used equations and a description of the uncertainty estimation are described in detail in the supplementary material (Appendix A).

4. Results

4.1. n-Alkane distributions

The *n*-alkanes of all sample types show a dominance of odd- over even-numbered homologues (Supplementary Table 1). ACL values range between 24 and 30 (Supplementary Table 1). The lowest ACL values were observed for submerged aquatic macrophytes (ACL of 24) and highest values were found for topsoil and terrestrial plant samples (both ACL of 29 to 30).

The *n*-alkane distributions of terrestrial plants (belonging to Poaceae, Juncaceae and a dwarf-shrub) show a predominance of the *n*-C_{29} and *n*-C_{31} alkanes (Fig. 2, Supplementary Table 1). The *n*-alkane distributions of dust trap and topsoil samples show a predominance of the long-chain (*n*-C_{29} and *n*-C_{31}) compounds (Fig. 2). In contrast, the samples from aquatic

macrophytes show a predominance of n-C_{23} and n-C_{25} alkanes with the latter occurring in slightly lower amounts (Fig. 2). Long-chain compounds occur only in low amounts in aquatic macrophyte samples. The aquatic moss sample shows a predominance of n-C_{27}. The exposed sediments and the two sediment traps from 30 and 90 m water depth apparently contain a mixture of n-alkanes from terrigenous and aquatic sources (Fig. 2) with n-C_{29} and n-C_{31} alkanes as the most abundant compounds. The surface sediment samples of LPA show on average a similar n-alkane distribution (Fig. 2) as sediment traps.

4.2. Compound-specific carbon isotope compositions

The $\delta^{13}C$ values for all n-alkanes range between -35.6 and -17.2‰ (Supplementary Table 2). In general, the aquatic plant samples exhibit the most enriched $\delta^{13}C$ values, while the dust traps and terrestrial plants show the lowest values (Fig. 2, Table 1). Isotopic values of the aquatic moss could not be determined due to too low compound abundance.

The terrestrial plants surrounding the lake show average $\delta^{13}C$ values for the n-C_{23} and n-C_{25} alkanes between -30.6 and -31.1‰. The n-C_{23} and n-C_{25} alkanes of the dust traps are slightly enriched (mean: -29.5 and -30.0‰) compared to terrestrial plants whereas topsoil sample PAT 44 shows very similar $\delta^{13}C$ values for n-C_{23} as terrestrial plants. This is the only $\delta^{13}C$ value (-30.4‰) for the mid-chain n-alkanes, which could be determined for the

topsoil samples due to low concentrations in these samples (Supplementary Table 2). The aquatic plants have the most enriched $\delta^{13}C$ values of all samples for mid-chain (around -18.0‰) *n*-alkanes. The sedimentary $\delta^{13}C$ values of *n*-C_{23} are enriched (mean: -23.4‰) relative to *n*-C_{25} (mean: -25.5‰). The sedimentary mid-chain *n*-alkanes are more enriched in $\delta^{13}C$ than the dust trap and terrestrial plant samples but similar to the material from the sediment traps. The exposed sediments show even more enriched values (-21.3 to -18.1‰) for the *n*-C_{23} alkane compared to the surface sediments (Supplementary Table 2, Fig. 2, Table 1).

The *n*-C_{29} and *n*-C_{31} alkanes of terrestrial plants show values between -31.4 and -31.2‰, respectively. The dust trap and topsoil samples show slightly depleted $\delta^{13}C$ values for *n*-C_{29} (mean: -33.3 for dust and -33.8‰ for soil) and for *n*-C_{31} (mean: -33.7 for dust and -33.8‰ for soil) compared to the terrestrial plants. The aquatic plant samples show also very enriched $\delta^{13}C$ values for long-chain (around -20.0‰) *n*-alkanes. The $\delta^{13}C$ values for the sedimentary long-chain *n*-alkanes average around -32.0‰. These values are very similar to those in sediment traps and exposed sediments but more enriched compared to $\delta^{13}C$ values of topsoil and dust trap samples.

4.3. Compound-specific hydrogen isotope compositions

The δD values of all *n*-alkanes range between -267 and -140‰ (Fig. 2, Supplementary Table 3). In general, the hydrogen isotope composition is

most enriched for aquatic plants and most depleted for terrestrial plants. In addition, long-chain *n*-alkanes (*n*-C_{29} and *n*-C_{31}) are more D-depleted than the mid-chain alkanes (*n*-C_{23} and *n*-C_{25}) (Fig. 2, Supplementary Table 3, Table 1), except for aquatic plants. Isotopic values of *n*-alkanes of the aquatic moss could not be determined.

δD of *n*-C_{23} could not be determined for some dust, topsoil and terrestrial plant samples due to too low abundance. The data show highly depleted δD values for the *n*-C_{23} alkane in dust (-222‰) and terrestrial plants (-207‰) compared to aquatic plant samples (average -171‰), (Table 1). Similar enriched values in δD of *n*-C_{23} alkanes were found in the sediment traps (average -174‰) as well as in surface sediments (average -177‰). The exposed sediments surrounding the lake show slightly more depleted values (average -182‰) compared to the surface sediments. δD of *n*-C_{25} alkanes show similar values as δD of *n*-C_{23} for terrestrial plants and sediment traps whereas δD values for *n*-C_{25} alkanes in the other sample groups show differences of 9 to 30‰ compared to the δD values of *n*-C_{23} (Supplementary Table 3).

δD compositions of long-chain *n*-alkanes are most D-depleted for terrestrial plants (around -250‰ on average), (Table 1). δD composition of the long-chain *n*-alkanes (*n*-C_{29} and *n*-C_{31}) in topsoil samples varies between -227 and -195‰ (Supplementary Table 3). The dust traps show more D-enriched values for the long-chain *n*-alkanes (-204‰ on average) compared to the topsoils. Similar δD values are exhibited by the sedimentary long-

chain *n*-alkanes (around -202‰). The sediment traps (-208‰ on average) and exposed sediments (-206‰ on average) show slightly more D-depleted values compared to surface sediments. δD of n-C_{27} shows for most of the samples intermediate values of mid- and long-chain *n*-alkanes.

5. Discussion

5.1. Identification of n-alkane sources

With regard to the *n*-alkane distribution of our samples (Fig. 2, Supplementary Table 1), the absence of *Sphagnum* mosses in the LPA catchment, and in accordance with other studies (Ficken et al., 2000; Mügler et al., 2008; Aichner et al., 2010a; Gao et al., 2011; Liu et al., 2015), we use the mid-chain *n*-alkane, n-C_{23}, as the representative for aquatic derived *n*-alkanes in the LPA sediment. The long-chain n-C_{29} alkane, being the most abundant homologue in the sediment, represents the terrestrial derived *n*-alkanes in our discussion.

The P_{aq} proxy (Ficken et al., 2000) allows for the evaluation of aquatic macrophyte *versus* terrestrial plant input to the lacustrine sediments (Table 1, Supplementary Table 1, see section 3.3.). The sediment traps and surface sediment samples show values ranging from 0.18 to 0.31, indicating mixed contributions by aquatic (mean of 0.81) and terrestrial plant material

(values between 0.04 and 0.18). The average chain length (ACL, see section 3.3) values also indicate mixed contributions (Supplementary Table 1).

To further disentangle the organic matter sources of n-C_{23} and n-C_{29}, we use the isotopic composition. Compound-specific $\delta^{13}C$ values of sediment traps and sediment samples show intermediate values (around -32‰) for the n-C_{29} alkane compared to the terrestrial plant (around -31.4‰) and topsoil/dust samples (around -33.8‰/-33.3‰), (Fig. 3b, Supplementary Table 2). The enriched $\delta^{13}C$ values of n-C_{29} in aquatic plants (average -20‰) thus seem to have a minor effect on $\delta^{13}C$ values of n-C_{29} alkanes in the sediments. Therefore, we infer that the $\delta^{13}C$ signature of n-C_{29} alkanes in sediment traps and sediments result from a mixture of terrestrial plant and dust or topsoil contributions.

The carbon isotopic values of n-C_{23} of aquatic plants are around -18‰. The $\delta^{13}C$ values of the n-C_{23} alkanes average around -22‰ for sediment traps and around -23‰ (Fig. 2, Fig. 3a, Supplementary Table 2) for surface sediment, indicating at least one additional source.

There are two possible explanations for the more depleted $\delta^{13}C$ signal in the sedimentary n-C_{23} alkanes compared to those in the aquatic plants. First, there could be a contribution of algae or aquatic mosses living in LPA and contributing to the sediment. Unfortunately, we were not able to measure compound-specific $\delta^{13}C$ or δD neither from algal material nor aquatic mosses from LPA. Besides, algae produce mainly short-chain n-alkanes (< C_{23}) and do not contribute large amounts of n-C_{23} alkanes to the

389 sediment (Cranwell et al., 1987; Meyers and Ishiwatari, 1993). Aquatic
390 mosses also produce n-C_{23} alkane (Fig. 2 and Supplementary Table 1),
391 however, a previous study inferred that the aquatic mosses do not
392 contribute a significant amount to OM in the modern LPA (Mayr et al.,
393 2009). This supports our assumption that the aquatic mosses have no
394 significant contribution to the sedimentary n-C_{23} alkanes under modern
395 conditions.

396 Other potential contributors of ^{13}C-depleted n-C_{23} alkanes to the LPA
397 sediment are terrestrial plants around the lake, windblown n-alkanes (dust)
398 or topsoils. $\delta^{13}C$ of n-C_{23} alkanes in most of the topsoil samples could not be
399 measured because of too low abundance (Supplementary Table 1). Only for
400 one topsoil sample (PAT 44) we were able to measure $\delta^{13}C$ of n-C_{23} (-30.4‰),
401 revealing similar values as for the terrestrial plants. Based on the very low
402 quantities of n-C_{23} alkanes in the topsoils samples, topsoils are not a likely
403 source of n-C_{23} alkanes in LPA sediments. Thus, the n-alkanes from
404 terrestrial plants surrounding the lake and from windblown n-alkanes
405 (dust) are possible additional sources explaining the depleted $\delta^{13}C$ signal of
406 n-C_{23} alkanes in the sediment.

407 The δD values of sedimentary n-C_{23} and n-C_{29} differ widely (about 30‰).
408 The large isotopic differences in δD values of long- and mid-chain n-alkanes
409 (Fig. 2) clearly indicate different hydrogen sources of aquatic and terrestrial
410 lipids. The δD values of n-C_{29} alkanes in sediments (mean: -205‰) are very
411 similar to δD values in dust traps (mean: -204‰) (Fig. 3b). This could be

either caused by a predominant contribution by dust, which is not supported by the sediment trap values (-210‰), or by a mixed contribution of all three identified *n*-alkane sources to the sediment. Dust is already a mixture of OM from different sources and transports, among others, plant leaf-waxes directly from plants, from distal topsoils or ablated past lake sediments to LPA sediments. Therefore, *n*-alkanes from topsoils are already an integrated part of the dust fraction. Based on this consideration, we infer dust, terrestrial and aquatic macrophytes as potential contributors of the sedimentary *n*-C_{29} alkanes.

Compound-specific δD of *n*-C_{23} alkanes of aquatic macrophytes show values around -171‰. The δD signal of *n*-C_{23} alkanes in sediment traps and sediments show slightly more depleted values (in average -174 and -177 ‰) (Fig. 3a). This difference in the hydrogen isotope signature can be explained by a contribution from another D-depleted source to the mid-chain *n*-alkane pool of LPA sediments as for instance terrestrial higher plants (Gao et al., 2011).

In summary, based on *n*-alkane distribution and isotopic compositions of mid- and long-chain *n*-alkanes of all measured samples (Fig. 3a, b), we identify aquatic and terrestrial plants as well as dust as the main *n*-alkane contributors to the LPA sediment. In order to achieve quantitative estimates of their relative contributions, we apply two different mixing models, i.e. one using the *n*-alkane distributions and one using their compound-specific isotope compositions. The results from these two models

are compared for verification and for identification of their strengths and weaknesses.

5.2. Model based on n-alkane distributions

To estimate to which extent the aquatic and two terrestrial sources contribute to the sedimentary *n*-alkane pool, we applied a quantitative approach based on *n*-alkane distribution following Gao et al. (2011). We modified this multi-source mixing (*n*-alkane distribution) model (see Material and Methods section) using site-specific end-members as described above, i.e., averaged *n*-alkane distributions of terrestrial plants, dust and aquatic plants. We applied the multi-source mixing model to sediment trap and surface sediment samples and obtained relative contributions from each source group to the sedimentary *n*-alkane pool. The averaged results based on this approach are shown in Fig. 4a.

According to the *n*-alkane distributions 62% (±9%) of the C_{23} *n*-alkane in LPA sediments originates from submerged aquatic plants, whereas, 35% (±8%) are delivered by dust and around 3% (±1%) are derived from terrestrial plants surrounding the lake (Fig. 4a, Table 2a). For the sedimentary *n*-C_{29} alkane this model indicates that terrestrial plants around the lake contribute 30% (±7%) and that 66% (±6%) are delivered by windblown dust. Only 5% (±2%) of the sedimentary *n*-C_{29} alkane is estimated to derive from aquatic plants. Uncertainties in source fraction

458 estimates for each individual sample (Table 2a) in the *n*-alkane distribution
459 model are proportional to the estimated values. These uncertainties are
460 caused by the combined effect of measurement errors and the diverging *n*-
461 alkane distribution patterns within each source group (Fig. 2,
462 Supplementary Table 1), which results in large initial uncertainties in end-
463 member distributions.

464 The results of the *n*-alkane distribution model show differences between
465 the sediment traps and the surface sediments (Fig. 4a, Table 2a). For
466 instance, the aquatic contribution is around 9% higher for the *n*-C_{23} alkane
467 in the sediment traps compared to surface sediment and the terrestrial
468 contribution is lower by the same amount (Fig. 4a, Table 2a), whereas the
469 aquatic contribution is 2% higher for the *n*-C_{29} alkanes in the sediment
470 traps and the terrestrial plant input is 10% lower in sediment trap material.
471 Considering the uncertainties of each estimated source fraction the aquatic
472 fraction shows no significant difference either for *n*-C_{23} or C_{29} while the
473 terrestrial fraction is different by at least 3% for *n*-C_{29} (see Table 2a:
474 terrestrial contribution for *n*-C_{29} of sediment traps 20% vs. sediment 30%
475 ±7). This small difference between the sediment traps and sediments for *n*-
476 C_{29} might be explained by degradation processes of OM in the water column
477 and sediments. Usually short-chain (< C_{23}) *n*-alkanes are preferentially
478 degraded in the water column (Cranwell, 1981; Robinson 1984) and are not
479 as resistant as mid-chain and long-chain *n*-alkanes. These data would thus
480 suggest that only the terrestrial fraction of *n*-C_{29} is affected by degradation.

However, degradation processes are not the only possible explanation for the observed differences. Alternatively, the difference between the sediment traps and sediments for n-C_{29} may be caused by the different temporal signal integration, i.e., 2 years for the sediment traps and 10 to 100 years for the surface sediment samples (Haberzettl et al., 2005; Kastner et al., 2010; Kliem et al., 2013). Instead of suggesting more extensive diagenetic degradation of long-chain n-alkanes it seems more plausible that the terrestrial input could have changed over the different time periods and caused the deviating results observed for sediment traps and sediments.

5.3. Model based on compound-specific isotopic composition

Unlike the n-alkane distributions (section 5.2), the compound-specific isotopic compositions provide additional environmental information to distinguish between n-alkanes from different sources and thus might serve better to estimate their relative contributions. We therefore developed a linear three-end-member mixing model based on the δD and $\delta^{13}C$ signals of the n-C_{23} and n-C_{29} alkanes to independently determine the relative contributions from dust, terrestrial and aquatic plants to the lake sediments.

The averaged results are shown in Figure 4b for sediment traps and surface sediments. All values are also shown in Table 2b including the estimated uncertainty of each individual sample. The results of the isotope

end-member mixing model show a significant contribution of mid-chain *n*-alkanes from submerged macrophytes to the lake sediments (Fig. 4b). The sedimentary *n*-C_{23} is composed of 73% (±12%) fractional input from submerged macrophytes, 19% (±9%) from terrestrial plants and 9% (±3%) from dust (Table 2b). The results from the sediment traps show a 2% higher aquatic contribution to *n*-C_{23} alkanes and a 3% lower terrestrial plant input compared to the results from surface sediments, which is within the calculated uncertainties and indicative for minor degradation processes in the water column.

For sedimentary *n*-C_{29} alkanes, the isotope mixing model suggests that 77% (±2%) are contributed by dust and 14% (±2%) are derived from terrestrial vegetation surrounding the lake (Fig. 4b, Table 2b). The model also suggests that around 9% (±1%) of the sedimentary *n*-C_{29} alkanes originate from aquatic plants. The sediment traps show 72% (±0%) windblown *n*-alkane contribution (dust) and 21% (±1%) terrestrial plant origin and 7% (±0%) aquatic contribution. The reasons mentioned above, i.e. degradation and different time intervals reflected by the samples (section 5.2), possibly account for the different estimates for *n*-C_{29} alkanes in the sediment traps and surface sediment samples. In general, however, our results indicate that degradation processes only have a minor effect on the isotopic composition of mid- and long-chain *n*-alkanes passing through the water column and being preserved in the sediment.

527 *5.4. Comparison of mixing models*

528

529 Both models yield consistent results regarding the major contributors of
530 n-C_{23} and n-C_{29} alkanes to the lake sediments, i.e., aquatic macrophytes for
531 n-$C_{23,}$ and wind-blown dust for n-C_{29}. There are, however, some
532 discrepancies regarding minor contributors, e.g. the n-alkane distribution
533 model suggests almost four times higher contribution from dust to the n-C_{23}
534 alkane pool and accordingly a lower terrestrial plant contribution (Tables
535 2a, b). In addition the terrestrial plant contribution suggested by the
536 distribution model is two times higher for n-C_{29} compared to the results of
537 the isotope model.

538 The differences between the results of the two models can be explained
539 by the different end-members used to disentangle the n-alkane sources. The
540 end-members of the isotope model include additional environmental
541 information and are clearly separated, while the n-alkane distribution
542 model uses averaged n-alkane patterns which are partly not significantly
543 different (i.e. terrestrial plants and dust, see Figure 2). This likely causes
544 the differences between the two models and leads to an overestimation of
545 some contributions in the n-alkane distribution model.

546 In this context, it should be noted that the fractional input predicted by
547 the isotope model for n-C_{23} has a relatively large spread especially in the
548 aquatic fraction (Tables 2a, b). The distribution model predicts a similar
549 pattern. This is likely due to the spatial heterogeneity in sedimentary n-C_{23}

at the lake floor and does not argue against the predictive power of the isotope model.

5.5. Implications for paleo-environmental reconstruction

In a previous study (Gao et al., 2011), the autochthonous input of mid-chain *n*-alkanes from aquatic plants to lake sediments in North America was found to be up to 90%. The amount of aquatic-derived n-C_{23} alkanes can, however, vary depending on local environmental conditions, amount of dust input for example, and needs to be quantified before being used for paleo-environmental reconstructions. For LPA sediment about three quarters of the n-C_{23} alkanes originate from aquatic macrophytes. Therefore, major changes in abundance and isotopic composition of sedimentary n-C_{23} alkanes at LPA should have been predominantly driven by past changes in the aquatic ecosystem and, in the case of carbon isotopes, by the imprint of contrasting isotopic signatures of dissolved CO_2 and HCO_3^- on the lacustrine primary producers (Mayr et al., 2009).

The main source of sedimentary n-C_{29} alkanes in LPA, on the other hand, is windblown material as indicated by both models. The exact origin of dust-derived *n*-alkanes cannot be identified without additional data. Due to dominating westerly winds in Southern Patagonia, the Andes and their foreland are the most likely source areas. A study on wind patterns (Mayr et al., 2007) may provide further constraints on potential dust source regions.

Strong winds mainly blow from a western and south-western direction to LPA. This suggests that n-C_{29} alkanes at LPA do not record a local but a regional paleo-vegetation and paleo-hydrologic signal. Pollen data showing that Andean pollen taxa as well as Patagonian steppe taxa occur in LPA sediments support this assumption (Schäbitz et al., 2003; Mayr et al., 2007). Therefore, it is likely that n-C_{29} alkanes of LPA sediments reflect an integrated environmental signal from the Patagonian steppe and forested areas closer to the Andes.

6. Summary and conclusions

This study presents distributions as well as carbon and hydrogen isotope compositions of n-alkanes from different organic matter sources in and around LPA and its surrounding area in Southern Patagonia and evaluates their use for paleo-environmental reconstructions. The investigated samples consist of terrestrial and aquatic plants, dust traps, topsoil samples, sediment traps as well as exposed and recent lake sediments from LPA. The n-C_{23} and n-C_{29} alkanes are used as indicators for autochthonous and allochthonous OM contributions to the lake sediments. Based on their compound-specific isotope compositions, we identified aquatic and terrestrial plants as well as dust as the main contributors to LPA sediments.

To quantify relative source contributions, two independent model approaches are used. One is based on *n*-alkane distributions and the other on their carbon and hydrogen isotopic compositions. Our study shows that the *n*-alkane distribution model as well as the isotope mixing model provides similar, within calculated uncertainties, estimates of the major *n*-alkane sources in the LPA sediment. Both approaches agree that more than two-thirds of recently deposited sedimentary n-C_{23} alkanes derive from aquatic marcophytes and should thus mainly record changes in isotopic compositions of lake waters. Sedimentary n-C_{29} alkanes, in contrast, are mainly derived from terrestrial sources with a dominant contribution by dust. Therefore, changes in its isotopic composition will reflect regional signals of vegetation and hydrology in southern Patagonia.

Acknowledgements:

We are grateful for research funding by the Deutsche Forschungsgemeinschaft (DFG) within the IODP/ICDP priority program - [Sche903/12 and Mo1416/7]. This research is also supported by the International Continental Scientific Drilling Program (ICDP) in the framework of the "Potrok Aike Maar Lake Sediment Archive Drilling Project" (PASADO). Funding for drilling was provided by the ICDP, the German Science Foundation (DFG), the Swiss National Funds (SNF), the Natural Sciences and Engineering Research Council of Canada (NSERC), the Swedish Vetenskapsradet (VR) and the University of Bremen. Sampling

was also carried out in the framework of DFG projects [MA 4235/4-1,-2] and [LU 786/7-1,-2].

For their invaluable help in field logistics and drilling we thank the staff of INTA Santa Cruz and Rio Dulce Catering as well as the Moreteau family and the DOSECC crew. We also thank Hendrik Grotheer and Ralph Kreutz for their help in the lab. We thank the editor Dr. Stefan Schouten and two anonymous reviewers for their comments and suggestions, which greatly improved the manuscript.

References

Aichner, B., Herzschuh, U., Wilkes, H., 2010a. Influence of aquatic macrophytes on the stable carbon isotopic signatures of sedimentary organic matter in lakes on the Tibetan Plateau. Organic Geochemistry 41, 706–718.

Aichner, B., Herzschuh, U., Wilkes, H., Vieth, A., Böhner, J., 2010b. δD values of n-alkanes in Tibetan lake sediments and aquatic macrophytes – A surface sediment study and application to a 16ka record from Lake Koucha. Organic Geochemistry 41, 779–790.

Anderson, R.F., Ali, S., Bradtmiller, L.I., Nielsen, S.H.H., Fleisher, M.Q., Anderson, B.E., Burckle, L.H., 2009. Wind-driven upwelling in the Southern Ocean and the deglacial rise in atmospheric CO2. Science 323, 1443–8.

Baas, M., Pancost, R., van Geel, B., Sinninghe Damsté, J.S., 2000. A comparative study of lipids in Sphagnum species. Organic Geochemistry 31, 535–541.

Bray, E.., Evans, E.., 1961. Distribution of n-paraffins as a clue to recognition of source beds. Geochimica et Cosmochimica Acta 22, 2–15.

Bush, R.T., McInerney, F.A., 2013. Leaf wax n-alkane distributions in and across modern plants: Implications for paleoecology and chemotaxonomy. Geochimica et Cosmochimica Acta 117, 161–179.

Cranwell, P.A., 1981. Diagenesis of free and bound lipids in terrestrial detritus deposited in a lacustrine sediment. Organic Geochemistry 3,

79–89.

Cranwell, P.A., Eglinton, G., Robinson, N., 1987. Lipids of aquatic organisms as potential contributors to lacustrine sediments—II. Organic Geochemistry 11, 513–527.

Dawson, T.E., Mambelli, S., Plamboeck, A.H., Templer, P.H., Tu, K.P., 2002. Stable Isotopes In Plant Ecology. Annual Review of Ecology and Systematics 33, 507–559.

Eglinton, G., Hamilton, R.J., 1967. Leaf epicuticular waxes. Science 156, 1322–1335.

Endlicher, W., 1993. Klimatische Aspekte der Weidedegradation in Ost-Patagonien, in: Hornetz, B., Zimmer, D. (Eds.), Beiträge Zur Kultur-Und Regionalgeographie. Festschrift Für Ralph Jätzold. pp. 91–103.

Ficken, K.J., Li, B., Swain, D.L., Eglinton, G., 2000. An n-alkane proxy for the sedimentary input of submerged/floating freshwater aquatic macrophytes. Organic Geochemistry 31, 745–749.

Gao, L., Hou, J., Toney, J., MacDonald, D., Huang, Y., 2011. Mathematical modeling of the aquatic macrophyte inputs of mid-chain n-alkyl lipids to lake sediments: Implications for interpreting compound specific hydrogen isotopic records. Geochimica et Cosmochimica Acta 75, 3781–3791.

Haberzettl, T., Fey, M., Lu, A., Maidana, N., Mayr, C., Ohlendorf, C., Scha, F., Schleser, G.H., Wille, M., 2005. Climatically induced lake level changes during the last two millennia as reflected in sediments of Laguna Potrok Aike , southern Patagonia (Santa. J. Paleolimnol. 33, 283–302.

Hueck K., Seibert P., 1981. Vegetationskarte von Südamerika. Springer-Verlag, Stuttgart.

Kastner, S., Ohlendorf, C., Haberzettl, T., Lücke, A., Mayr, C., Maidana, N.I., Schäbitz, F., Zolitschka, B., 2010. Southern hemispheric westerlies control the spatial distribution of modern sediments in Laguna Potrok Aike, Argentina. Journal of Paleolimnology 44, 887–902.

Kliem, P., Enters, D., Hahn, A., Ohlendorf, C., Lisé-Pronovost, A., St-Onge, G., Wastegård, S., Zolitschka, B., 2013. Lithology, radiocarbon chronology and sedimentological interpretation of the lacustrine record from Laguna Potrok Aike, southern Patagonia. Quaternary Science Reviews 71, 54–69.

Liu, W., Yang, H., Wang, H., An, Z., Wang, Z., Leng, Q., 2015. Carbon isotope composition of long chain leaf wax n-alkanes in lake sediments: A dual indicator of paleoenvironment in the Qinghai-Tibet Plateau. Organic Geochemistry 83–84, 190–201.

Magill, C.R., Ashley, G.M., Freeman, K.H., 2013. Ecosystem variability and early human habitats in eastern Africa. Proceedings of the National Academy of Sciences 110, 1167–1174.

Massaferro, J., Recasens, C., Larocque-Tobler, I., Zolitschka, B., Maidana, N.I.I., 2012. Major lake level fluctuations and climate changes for the past 16,000 years as reflected by diatoms and chironomids preserved in the sediment of Laguna Potrok Aike, southern Patagonia. Quaternary Science Reviews 71, 1–8.

Mayr, C., Lücke, A., Maidana, N.I., Wille, M., Haberzettl, T., Corbella, H., Ohlendorf, C., Schäbitz, F., Fey, M., Janssen, S., Zolitschka, B., 2009. Isotopic fingerprints on lacustrine organic matter from Laguna Potrok Aike (southern Patagonia, Argentina) reflect environmental changes during the last 16,000 years. Journal of Paleolimnology 42, 81–102.

Mayr, C., Lücke, A., Stichler, W., Trimborn, P., Ercolano, B., Oliva, G., Ohlendorf, C., Soto, J., Fey, M., Haberzettl, T., Janssen, S., Schäbitz, F., Schleser, G.H., Wille, M., Zolitschka, B., 2007. Precipitation origin and evaporation of lakes in semi-arid Patagonia (Argentina) inferred from stable isotopes (δ18O, δ2H). Journal of Hydrology 334, 53–63.

Mayr, C., Lucke, a., Wagner, S., Wissel, H., Ohlendorf, C., Haberzettl, T., Oehlerich, M., Schabitz, F., Wille, M., Zhu, J., Zolitschka, B., 2013. Intensified Southern Hemisphere Westerlies regulated atmospheric CO2 during the last deglaciation. Geology 41, 831–834.

Meyers, P.A., Ishiwatari, R., 1993. Lacustrine organic geochemistry—an overview of indicators of organic matter sources and diagenesis in lake sediments. Organic Geochemistry 20, 867–900.

Moore, D.M., 1983. Flora of Tierra del Fuego. Anthony Nelson-Missouri Botanical Garden, Saint Louis.

Mügler, I., Gleixner, G., Günther, F., Mäusbacher, R., Daut, G., Schütt, B., Berking, J., Schwalb, a., Schwark, L., Xu, B., Yao, T., Zhu, L., Yi, C., 2009. A multi-proxy approach to reconstruct hydrological changes and Holocene climate development of Nam Co, Central Tibet. Journal of Paleolimnology 43, 625–648.

Mügler, I., Sachse, D., Werner, M., Xu, B., Wu, G., Yao, T., Gleixner, G., 2008. Effect of lake evaporation on δD values of lacustrine n-alkanes: A comparison of Nam Co (Tibetan Plateau) and Holzmaar (Germany). Organic Geochemistry 39, 711–729.

Oehlerich, M., Mayr, C., Gussone, N., Hahn, a., Hölzl, S., Lücke, a., Ohlendorf, C., Rummel, S., Teichert, B.M. a., Zolitschka, B., 2015. Lateglacial and Holocene climatic changes in south-eastern Patagonia inferred from carbonate isotope records of Laguna Potrok Aike (Argentina). Quaternary Science Reviews 114, 189–202.

Ohlendorf, C., Fey, M., Gebhardt, C., Haberzettl, T., Lücke, A., Mayr, C., Schäbitz, F., Wille, M., Zolitschka, B., 2013. Mechanisms of lake-level change at Laguna Potrok Aike (Argentina) – insights from hydrological balance calculations. Quaternary Science Reviews 71, 27–45.

Peri, P.L., Lencinas, M.V., Pastur, G.M., Wardell-johnson, G.W., 2013. Diversity Patterns in the Steppe of Aregentinian Southern Patagonia: Environmental Drivers and Impact of Grazing. Steppe Ecosystems 332, 73–95.

Pfadenhauer, J., Klötzli, F., 2015. Vegetation der Erde: Grundlagen, Ökologie, Verbreitung. Springer-Verlag.

Poynter, J.G., Farrimond, P., Robinson, N., Eglinton, G., 1989. Aeolian-Derived Higher Plant Lipids in the Marine Sedimentary Record: Links with Palaeoclimate, in: Leinen, M., Sarnthein, M. (Eds.), Paleoclimatology and Paleometeorology: Modern and Past Patterns of Global Atmospheric Transport SE - 18, NATO ASI Series. Springer Netherlands, pp. 435–462.

Recasens, C., Ariztegui, D., Maidana, N.I., Zolitschka, B., 2015. Diatoms as indicators of hydrological and climatic changes in Laguna Potrok Aike (Patagonia) since the Late Pleistocene. Palaeogeography, Palaeoclimatology, Palaeoecology 417, 309–319.

Robinson, N., Cranwell, P.A., Finlay, B.J., Eglinton, G., 1984. Lipids of aquatic organisms as potential contributors to lacustrine sediments. Organic Geochemistry 6, 143–152.

Roig, F., 1998. La Vegetación de la Patagonia, in: Correa, M. Flora Patagónica, Tomo VIII, Vol. 1. INTA Colección Científica, Buenos Aires, pp. 48–174.

Sachse, D., Billault, I., Bowen, G.J., Chikaraishi, Y., Dawson, T.E., Feakins, S.J., Freeman, K.H., Magill, C.R., McInerney, F. a., van der Meer, M.T.J., Polissar, P., Robins, R.J., Sachs, J.P., Schmidt, H.-L., Sessions, A.L., White, J.W.C., West, J.B., Kahmen, A., 2012. Molecular Paleohydrology: Interpreting the Hydrogen-Isotopic Composition of Lipid Biomarkers from Photosynthesizing Organisms. Annual Review of Earth and Planetary Sciences 40, 221–249.

Sachse, D., Radke, J., Gleixner, G., 2004. Hydrogen isotope ratios of recent lacustrine sedimentary n-alkanes record modern climate variability. Geochimica et Cosmochimica Acta 68, 4877–4889.

Schäbitz, F., Paez, M., Mancini, M., Quintana, F., Wille, M., Corbella, H., Haberzettl, T., Lücke, A., Prieto, A., Maidana, N., Mayr, C., Ohlendorf, C., Schleser, G., Zolitschka, B., 2003. Estudios paleoambientales en lagos volcánicos en la Región Volcánica de Pali Aike, sur de Patagonia (Argentina): palinología. Rev. del Mus. Argentino Ciencias Nat. nueva Ser.

Schäbitz, F., Wille, M., Francois, J.P., Haberzettl, T., Quintana, F., Mayr, C., Lücke, A., Ohlendorf, C., Mancini, V., Paez, M.M., Prieto, A.R., Zolitschka, B., 2013. Reconstruction of palaeoprecipitation based on pollen transfer functions - the record of the last 16ka from Laguna Potrok Aike, southern Patagonia. Quaternary Science Reviews 71, 175–190.

Schefuss, E., Schouten, S., Schneider, R.R., 2005. Climatic controls on central African hydrology during the past 20,000 years. Nature 437, 1003–6.

Schmidt, F., Oberhänsli, H., Wilkes, H., 2014. Biocoenosis response to hydrological variability in Southern Africa during the last 84kaBP: A study of lipid biomarkers and compound-specific stable carbon and hydrogen isotopes from the hypersaline Lake Tswaing. Global and Planetary Change 112, 92–104.

The Nature Conservancy, 2009. URL: http://maps.tnc.org/gis_data.html, last accessed: September 20, 2016; Glob. Ecoregions, Major Habitat Types, Biogeogr. Realms Nat. Conserv. Terr. Assess. Units as December 14, 2009.

Wille, M., Maidana, N.I., Schäbitz, F., Fey, M., Haberzettl, T., Janssen, S., Lücke, A., Mayr, C., Ohlendorf, C., Schleser, G.H., Zolitschka, B., 2007. Vegetation and climate dynamics in southern South America: The microfossil record of Laguna Potrok Aike, Santa Cruz, Argentina. Review of Palaeobotany and Palynology 146, 234–246.

Zhu, J., Lücke, A., Wissel, H., Mayr, C., Enters, D., Ja Kim, K., Ohlendorf, C., Sch??bitz, F., Zolitschka, B., 2014. Climate history of the Southern Hemisphere Westerlies belt during the last glacial-interglacial transition revealed from lake water oxygen isotope reconstruction of Laguna Potrok Aike (52° S, Argentina). Climate of the Past Discussions 10, 2153–2169.

Zhu, Lücke, A., Wissel, H., Müller, D., Mayr, C., Ohlendorf, C., Zolitschka, B., 2013. The last Glacial-Interglacial transition in Patagonia, Argentina: The stable isotope record of bulk sedimentary organic matter from Laguna Potrok Aike. Quaternary Science Reviews 71, 205–218.

Zimmermann, C., Jouve, G., Pienitz, R., Francus, P., Maidana, N.I., 2015. Late Glacial and Early Holocene cyclic changes in paleowind conditions and lake levels inferred from diatom assemblage shifts in Laguna Potrok Aike sediments (southern Patagonia, Argentina). Palaeogeography, Palaeoclimatology, Palaeoecology 427, 20–31.

Zolitschka, B., Anselmetti, F., Ariztegui, D., Corbella, H., Francus, P., Lücke, A., Maidana, N.I., Ohlendorf, C., Schäbitz, F., Wastegård, S., 2013. Environment and climate of the last 51,000 years – new insights

from the Potrok Aike maar lake Sediment Archive Drilling prOject (PASADO). Quaternary Science Reviews 71, 1–12.

Zolitschka, B., Schäbitz, F., Lücke, A., Corbella, H., Ercolano, B., Fey, M., Haberzettl, T., Janssen, S., Maidana, N., Mayr, C., Ohlendorf, C., Oliva, G., Paez, M.M., Schleser, G.H., Soto, J., Tiberi, P., Wille, M., 2006. Crater lakes of the Pali Aike Volcanic Field as key sites for paleoclimatic and paleoecological reconstructions in southern Patagonia, Argentina. Journal of South American Earth Sciences 21, 294–309.

Figures and Tables:

Fig. 1: Sampling sites and terrestrial ecoregions (The Nature Conservancy; http://maps.tnc.org/gis_data.html) in Southern Patagonia, Argentina. a) Sampling sites of the topsoil transect from Rio Gallegos to Rio Turbio (1-16), locations of the pollen trap samples (PT), one terrestrial plant sampling site (PAT 16) and the location of LPA. b) Bathymetric map of LPA with sampling sites surrounding the lake (PAT and PAIS), plant sampling sites (not indicated), locations of the sediment trap mooring (ST) and sites of surface sediments. Map created with QGIS (qgis.org)..

Fig. 2: Histograms of normalized *n*-alkane distributions (terrestrial plants = green bars; dust traps = golden bars; topsoils = brown bars; exposed sediments grey-blue bars; aquatic plants and aquatic moss = blue bars; sediment traps and surface sediments = grey bars) show averaged distribution values with mean standard deviation of each sample group including n samples, overlain by averaged stable carbon and hydrogen

isotope data for individual homologues. Error bars for $\delta^{13}C$ and δD values are not shown (Supplementary Table 2). Terrestrial samples show high relative amounts of long-chain *n*-alkanes and low $\delta^{13}C$ as well as δD values, while aquatic samples show high relative amounts of mid-chain *n*-alkanes and relatively high $\delta^{13}C$ as well as δD values. Note that all y-axes are standardized, except for the terrestrial plants and aquatic marcopytes (1 and 0.5 instead of 0.4 for the normalized *n*-alkane content). Isotopic values of the aquatic moss sample could not be determined.

Fig. 3: Cross plots showing δD and $\delta^{13}C$ values of n-C_{23} and n-C_{29} alkanes in potential source samples and sediments. Grey symbols indicate single values and coloured ones are the mean values of each source group. a) Cross plot for n-C_{23} alkanes showing that sedimentary n-C_{23} alkanes plot close to aquatic plant samples. b) Cross plot for n-C_{29} alkanes showing that sedimentary n-C_{29} alkanes reveal similar isotopic values as dust and topsoil samples.

Fig 4: Bar charts showing relative source contributions to n-C_{23} and n-C_{29} alkanes to the sediment (blue = aquatic plants, green = terrestrial plants, gold = dust). a) Fractional contributions based on the *n*-alkane distribution model. b) Fractional contributions based on the isotope model.

Table 1: Mean $\delta^{13}C$ and δD values and standard deviations (sd) of *n*-C_{23} to *n*-C_{31} alkanes and Paq and ACL values from all sample groups (n.a. = not available). Standard deviations of averages are based on individual isotope values. * Single value

Table 2: Results of a) the *n*-alkane distribution model and b) the isotope end-member-mixing model, showing fractional contributions of aquatic plants (aqua), terrestrial plants (terr) and dust to the *n*-alkane pool in sediment traps and sediments of LPA, including standard deviations (sd) of each fractional contribution and for each sample. Standard deviations are based on individual fractional estimates (n.a. = not avaiable).

Supplementary Tables:

Supplementary Table 1: Sample description and location, collection dates, coordinates, P_{aq}, average chain length (ACL), carbon preference index (CPI) and individual *n*-alkane concentrations (n.a. = not available, n.d. = not detected).

[a] $ACL = \sum(C_n*n)/\sum C_n$; (Poynter et al., 1989)

[b] $CPI = 0.5*(\sum_{odd}C_{23–33}/\sum_{even}C_{22–3}) + (\sum_{odd}C_{23–33}/\sum_{even}C_{24–34})$; (Bray and Evans, 1961)

Supplementary Table 2: Mean $\delta^{13}C$ values and standard deviations (sd) of *n*-C_{23} to *n*-C_{33} alkanes from all samples (n.a. = not available, n.d. = not detected). Standard deviations of averages are based on individual isotope values. * Single value

Supplementary Table 3: Mean δD values and standard deviations (sd) of *n*-C_{23} to *n*-C_{33} alkanes from all samples (n.a. = not available n.d. = not detected). Standard deviations of averages are based on individual isotope values.

* Single value

Figure

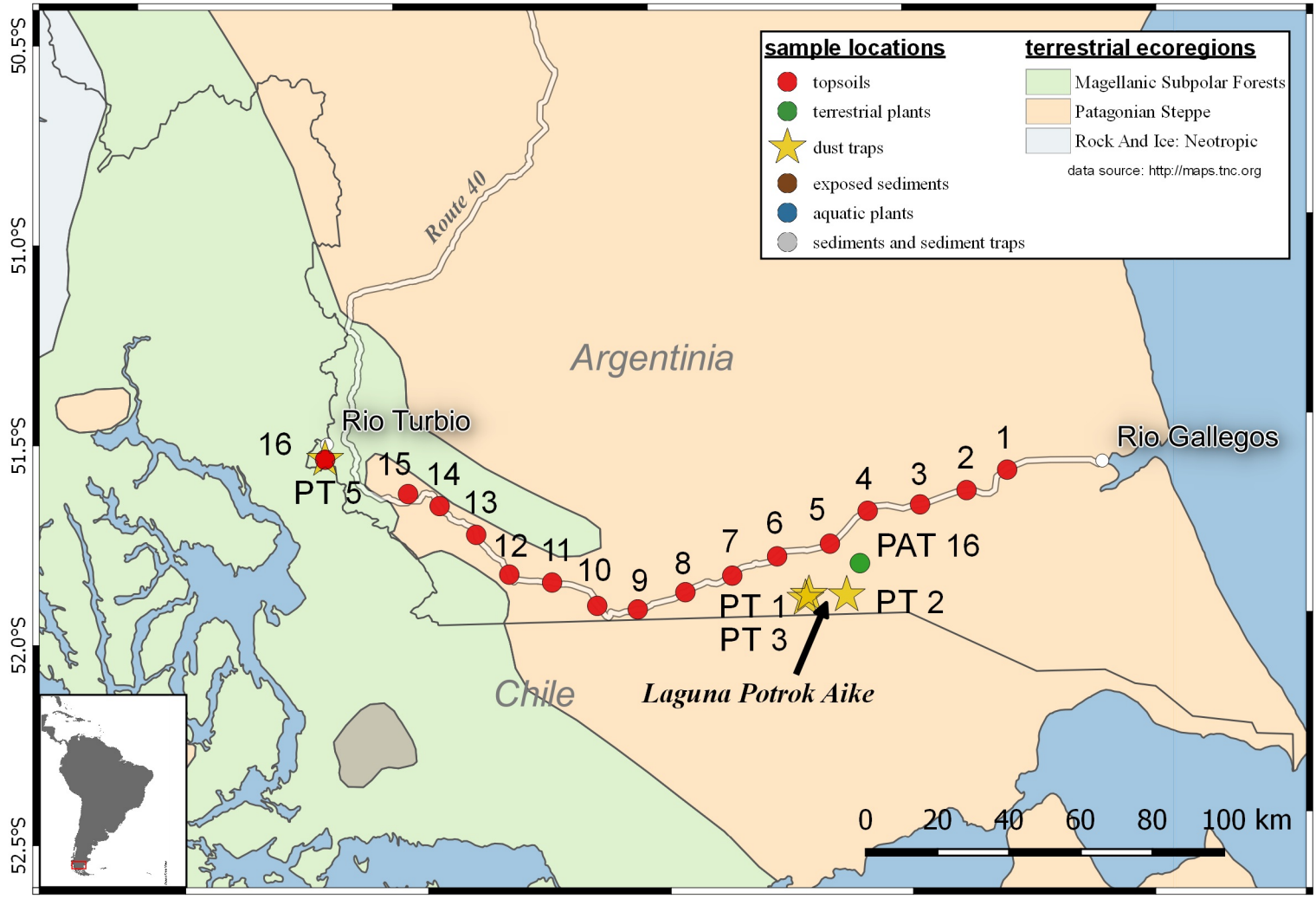
73.0°W
72.0°W
71.0°W
70.0°W
69.0°W
50.5°S
51.0°S
51.5°S
52.0°S
52.5°S
sample locations
topsoils
terrestrial plants
dust traps
exposed sediments
aquatic plants
sediments and sediment traps
terrestrial ecoregions
Magellanic Subpolar Forests
Patagonian Steppe
Rock And Ice: Neotropic
data source: http://maps.tnc.org
Route 40
Argentinia
Chile
Rio Turbio
Rio Gallegos
Laguna Potrok Aike
1
2
3
4
5
6
7
8
9
10
11
12
13
14
15
16
PT 5
PT 1
PT 3
PT 2
PAT 16
0
20
40
60
80
100 km

Figure

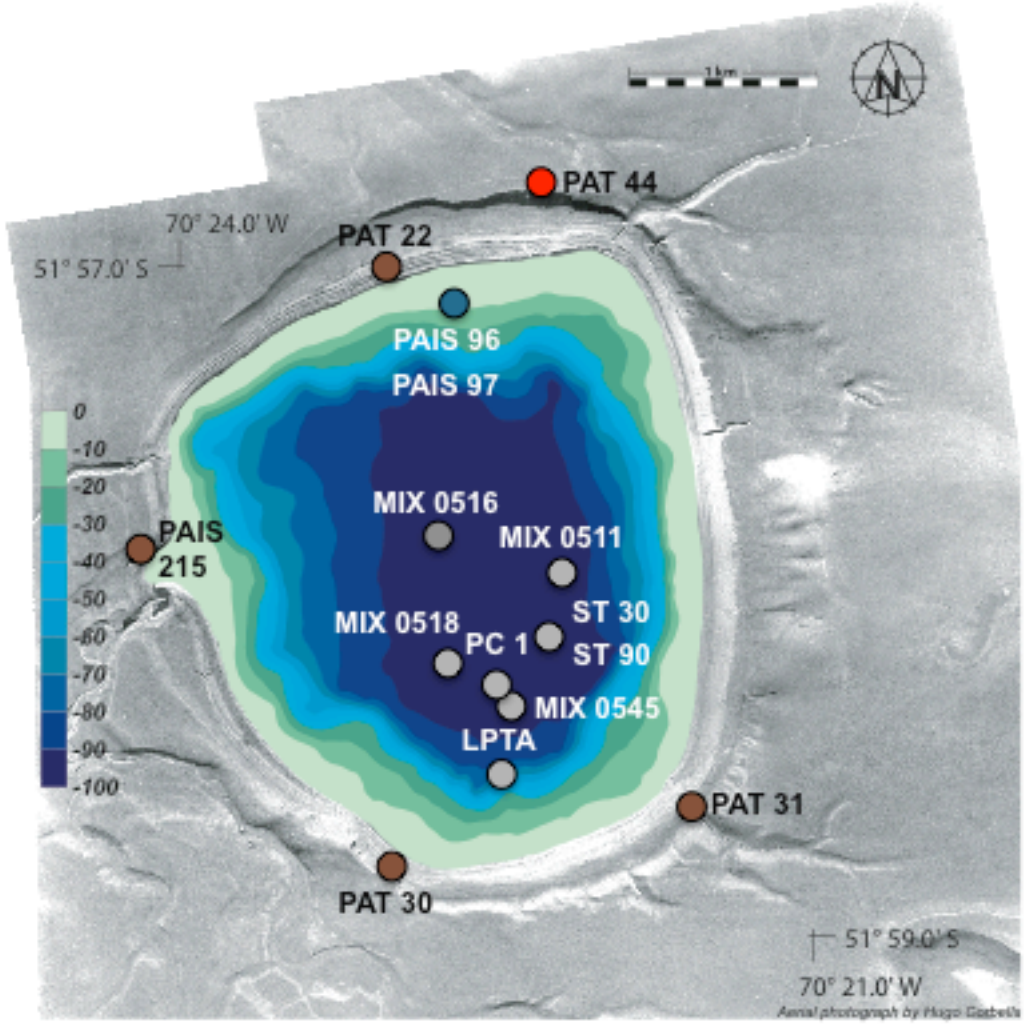
1km
N
PAT 44
70° 24.0' W
PAT 22
51° 57.0' S
PAIS 96
PAIS 97
0
-10
-20
-30
-40
-50
-60
-70
-80
-90
-100
MIX 0516
MIX 0511
PAIS
215
ST 30
MIX 0518
PC 1
ST 90
MIX 0545
LPTA
PAT 31
PAT 30
51° 59.0' S
70° 21.0' W
Aerial photograph by Hugo Gabella

Figure 5

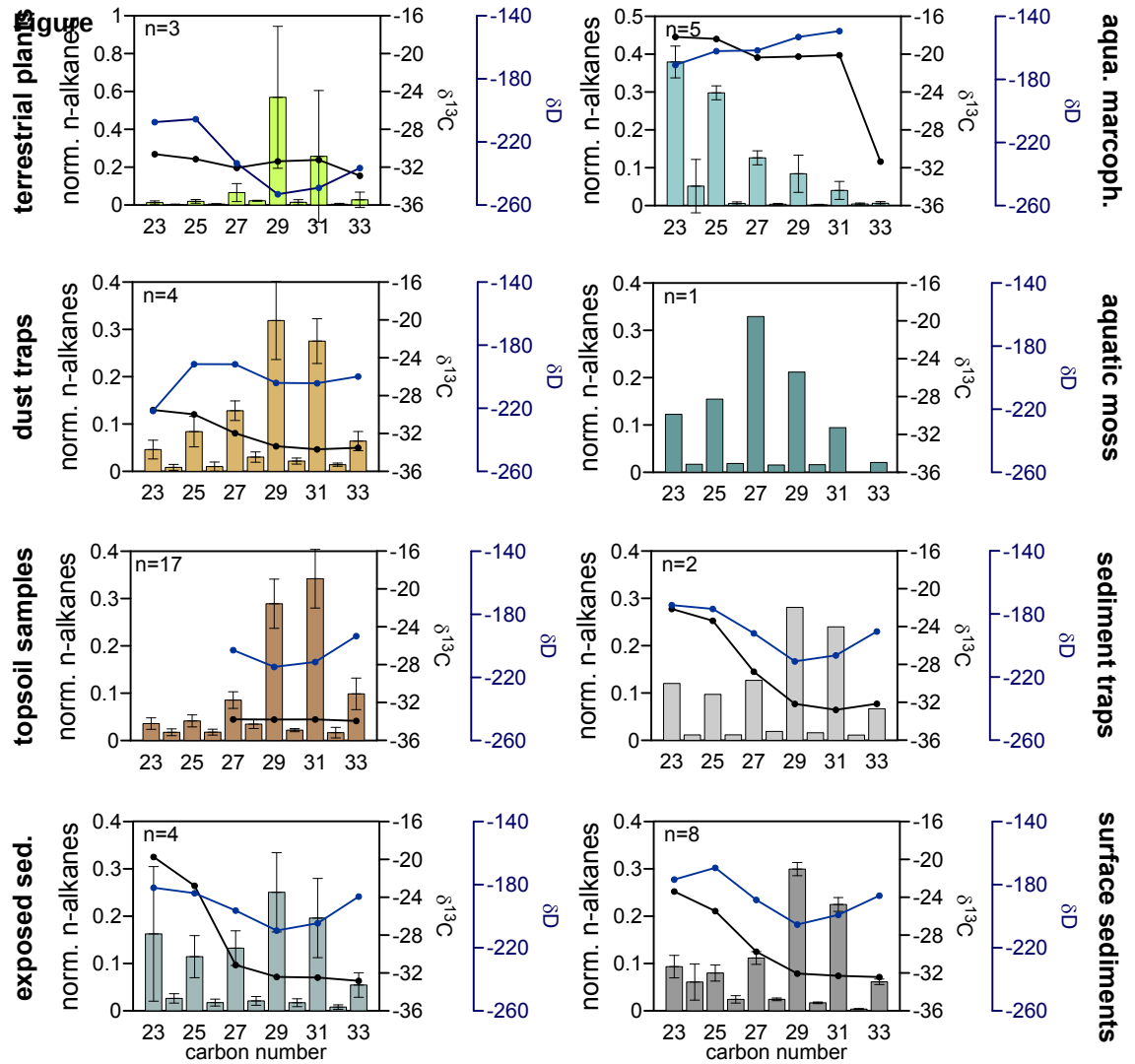
terrestrial plants
n=3
aqua. marcoph.
n=5
dust traps
n=4
aquatic moss
n=1
topsoil samples
n=17
sediment traps
n=2
exposed sed.
n=4
surface sediments
n=8
norm. n-alkanes
δ13C
δD
carbon number
23 25 27 29 31 33

Figure

a)

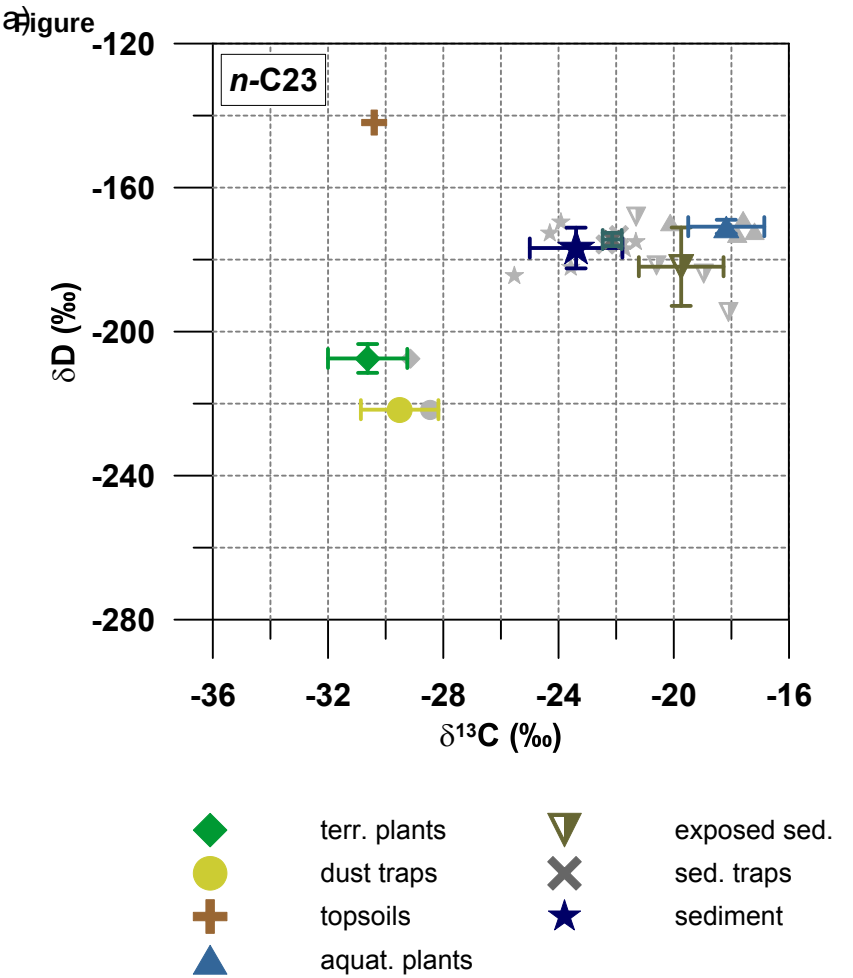
n-C23
-120
-160
-200
-240
-280
δD (‰)
-36
-32
-28
-24
-20
-16
δ13C (‰)
terr. plants
dust traps
topsoils
aquat. plants
exposed sed.
sed. traps
sediment

b)

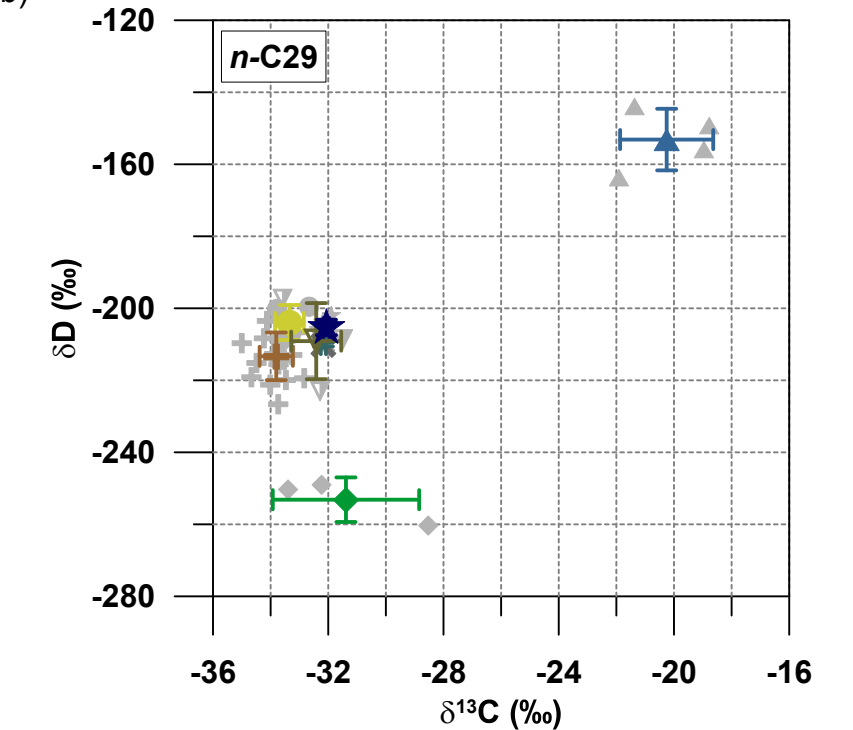
n-C29
-120
-160
-200
-240
-280
δD (‰)
-36
-32
-28
-24
-20
-16
δ13C (‰)

Figure 5

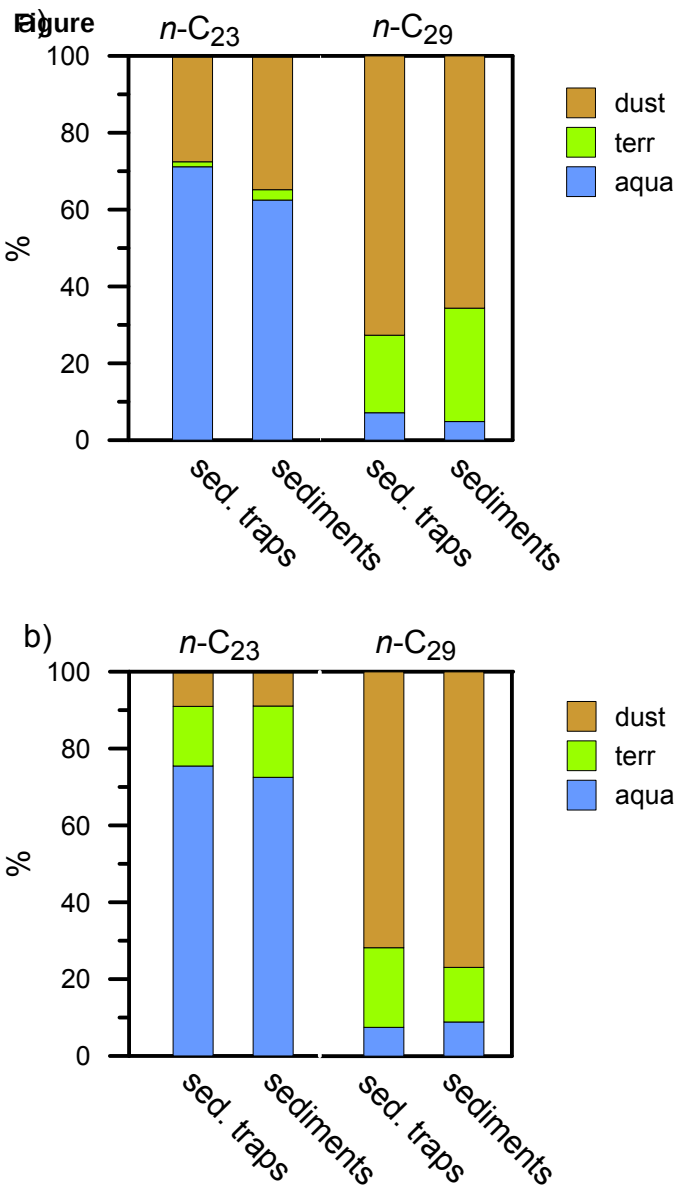
a)
n-C23
n-C29
100
80
60
40
20
0
%
dust
terr
aqua
sed. traps
sediments
sed. traps
sediments
b)
n-C23
n-C29
100
80
60
40
20
0
%
dust
terr
aqua
sed. traps
sediments
sed. traps
sediments

Table

sample groups	sample number	Paq	ACL (23-33)	δD *n*C23	sd	δD *n*C25	sd	δD *n*C27	sd	δD *n*C29	sd	δD *n*C31	sd	δ13C *n*C23	sd	δ13C *n*C25	sd	δ13C *n*C27	sd	δ13C *n*C29	sd	δ13C *n*C31	sd
terrestrial plants	3	0.04	29	-207*	n.a.	-206	13	-234	4	-253	6	-249	15	-30.6	1.4	-31.1	1.0	-32.1	1.6	-31.4	2.5	-31.2	2.1
dust traps	4	0.18	29	-222*	n.a.	-192	18	-192	8	-204	5	-204	18	-29.5	1.3	-30.0	1.3	-32.0	1.2	-33.3	0.5	-33.7	0.2
topsoils	17	0.11	29	-142*	n.a.	-178*	n.a	-203	6	-213	7	-210	8	-30.4*	n.a	-31.4*	n.a	-33.8	0.7	-33.8	0.6	-33.8	0.7
exposed sediments	4	0.41	28	-182	11	-185	5	-196	3	-209	11	-204	8	-19.7	1.5	-22.8	2.0	-31.2	1.6	-32.4	0.9	-32.5	1.1
aquatic plants	4	0.81	26	-171	2	-162	1	-162	7	-153	9	-149	10	-18.2	1.3	-18.4	1.3	-20.4	2.1	-20.3	1.6	-20.1	1.2
sediment traps	2	0.30	28	-174	2	-177	1	-192	1	-210	1	-206	1	-22.1	0.3	-23.4	0.5	-28.8	0.1	-32.2	0.1	-32.8	0.0
surface sediments	6	0.26	28	-177	6	-169	0	-190	7	-205	2	-199	1	-23.4	1.6	-25.5	1,.5	-29.7	0.9	-32.1	0.1	-32.3	0.2

Table

Tab. 2a:

	fraction input of *n*-C23						fraction input of *n*-C29					
Site	aqua	sd	terr	sd	dust	sd	aqua	sd	terr	sd	dust	sd
ST 30	72	13	1	2	27	13	7	4	21	16	72	17
ST 90	71	14	1	2	28	14	7	4	19	16	74	16
mean ST	**71**	**n.a.**	**1**	**n.a.**	**28**	**n.a.**	**7**	**n.a.**	**20**	**n.a.**	**73**	**n.a.**
LPA	65	16	2	2	33	16	5	3	21	16	73	16
PC 1	73	13	1	2	25	13	8	4	23	17	70	17
Mix0511	69	17	3	3	28	17	5	3	37	20	57	21
Mix0516	62	18	3	3	35	19	5	3	29	19	66	19
Mix0518	47	23	4	5	49	24	2	2	34	20	64	20
Mix0545	58	20	3	4	38	20	4	3	34	19	63	20
mean Sed.	**62**	**9**	**3**	**1**	**35**	**8**	**5**	**2**	**30**	**7**	**66**	**6**

Tab. 2b:

	fraction input of *n*-C23						fraction input of *n*-C29					
Site	aqua	sd	terr	sd	dust	sd	aqua	sd	terr	sd	dust	sd
ST 30	72	6	18	10	11	8	7	4	21	11	72	13
ST 90	79	7	13	8	7	6	8	5	20	10	72	12
mean ST	**75**	**n.a.**	**16**	**n.a.**	**9**	**n.a.**	**7**	**n.a.**	**21**	**n.a.**	**72**	**n.a.**
LPA	77	6	14	8	9	6	11	4	11	7	78	9
PC 1	82	6	11	7	7	5	9	4	14	8	77	10
Mix0511	62	7	25	12	13	9	8	4	12	7	80	9
Mix0516	83	6	11	7	6	4	9	4	15	8	76	11
Mix0518	53	6	35	13	12	10	8	4	17	9	75	11
Mix0545	78	7	15	9	7	5	9	4	16	9	75	11
mean Sed.	**73**	**12**	**19**	**9**	**9**	**3**	**9**	**1**	**14**	**2**	**77**	**2**